HHS Public Access

Author manuscript

J Immunol. Author manuscript; available in PMC 2024 October 15.

Published in final edited form as:

J Immunol. 2023 October 15; 211(8): 1203–1215. doi:10.4049/jimmunol.2200473.

Sec22b and Stx4-depletion has no major effect on cross-presentation of PLGA microsphere-encapsulated antigen and a synthetic long peptide *in vitro*

Emma G.M. Tondeur[*], **Jane S.A. Voerman**[*], **Mitchell A.A. Geleijnse**[*], **Laure S. van Hofwegen**[*], **Anneloes van Krimpen**[*], **Julia Koerner**[†], **Gunja Mishra**[*], **Ziye Song**[*], **Christopher Schliehe**[*,‡]

[*]Department of Immunology, Erasmus MC, University Medical Center Rotterdam, Rotterdam, The Netherlands

[†]Division of Immunology, Department of Biology, University of Konstanz, Konstanz, Germany

Abstract

The induction of cytotoxic T-lymphocyte (CTLs) responses by vaccines is important to combat infectious diseases and cancer. Biodegradable poly(lactic-*co*-glycolic acid) (PLGA) microspheres (MS) and synthetic long peptides (SLPs) are efficiently internalized by professional antigen presenting cells (APCs) and prime CTL responses after cross-presentation of antigens on major histocompatibility complex (MHC) class I molecules. Specifically, they mainly utilize the cytosolic pathway of cross-presentation that requires endosomal escape, proteasomal processing, and subsequent MHC class I loading of antigens in the endoplasmic reticulum (ER) and/or the endosome. The v-SNARE protein Sec22b has been described as important for this pathway by mediating vesical trafficking for the delivery of ER-derived proteins to the endosome. As this function has also been challenged, we investigated the role of Sec22b in cross-presentation of the PLGA-MS-encapsulated model antigen ovalbumin and a related SLP. Using CRISPR/Cas9-mediated genome editing, we generated Sec22b knockouts (KOs) in two murine C57BL/6-derived APC lines and found no evidence for an essential role of Sec22b. Although pending experimental evidence, the t-SNARE protein syntaxin-4 (Stx4) has been suggested to promote cross-presentation by interacting with Sec22b for the fusion of ER-derived vesicles with the endosome. We show here that, similar to Sec22b, Stx4 KO in murine APCs had very limited effects on cross-presentation under the conditions tested here. This study contributes to characterizing cross-presentation of two promising antigen delivery systems and adds to the discussion about the role of Sec22b/Stx4 in related pathways. Our data point towards SNARE protein redundancy in the cytosolic pathway of cross-presentation.

Introduction

Therapeutic vaccines that induce potent cytotoxic T-cell (CTL) responses are of crucial importance for immunotherapy of cancer (1). CTLs can kill their target cells after recognition of endogenous peptides that are presented on major histocompatibility complex

[‡]Corresponding author. Tel. +31-1070-43188; c.schliehe@erasmusmc.nl.

(MHC) class I molecules via the direct presentation pathway (2). To acquire their full CTL effector functions, naïve $CD8^+$ T-cells need initial priming by professional antigen presenting cells (APCs), such as dendritic cells (DCs) and macrophages (3, 4). APCs can present MHC class I-associated peptides in combination with co-stimulatory signals after their activation by pathogen- or danger-associated molecular patterns (PAMPs, DAMPs) - a mechanism exploited by adjuvants in vaccine formulations (5). Besides the direct presentation of endogenous antigens, APCs have the unique property to present peptides derived from exogenous sources in the context of MHC class I (3, 4). This process is referred to as `cross-presentatioń and represents the exclusive pathway by which CTLs can be primed against tissue-specific antigens, such as those present in cancer or antigens associated with intracellular pathogens that either do not infect APCs or interfere with the direct presentation pathway (3, 6).

In general, cross-presentation takes place after endocytosis of exogenous antigens, after which internalized cargo reaches the endosomal compartment. From here, antigens can follow two distinct cross-presentation pathways (3, 4). In the vacuolar pathway, antigens are processed by lysosomal proteases in an endo/lysosomal compartment after acidification, in which generated peptides are also loaded onto MHC class I molecules for cell surface presentation (3, 4). In the cytosolic pathway, antigens leave the endosome via an ER-associated protein degradation (ERAD)-associated protein translocon to the cytoplasm and are degraded into peptides by the proteasome (7, 8). Next, generated peptides can again follow two distinct routes: In the phagosome-to-cytosol (P2C) pathway, antigens enter the direct presentation pathway via ER and Golgi (3, 4, 6). Alternatively, in the phagosome-to-cytosol-to-phagosome (P2C2P) pathway, the peptides are transported back into the endosome by the transporter associated with antigen processing (TAP) and are then loaded on MHC class I inside the endosomal compartment (6). In both cases, the MHC class I/peptide complexes are then transported to the surface for cross-priming of CTLs.

In the cytosolic pathway, the delivery of ER-resident proteins of the ERAD machinery (such as the translocon Sec61/p97), the TAP transporter, and components of the peptide loading complex (PLC) to the endosomes is essential for efficient cross-presentation. There is general consensus that this delivery occurs via an ER-Golgi intermediate compartment (ERGIC), which is normally known for trafficking proteins from the ER to the Golgi (4, 9, 10). The fusion between ERGIC vesicles and the endosome is mediated by SNARE (soluble N-ethylmaleimide-sensitive factor attachment protein receptor) proteins, present on both the ERGIC and the endosomal membrane (11). It has previously been suggested that the vesicle (v)-SNARE protein Sec22b is crucial for the endosomal delivery of ER-resident proteins for efficient cross-presentation (9, 10, 12, 13). However, this role of Sec22b remains controversial, as it has also been challenged (14). Interestingly, in current literature the target (t)-SNARE protein syntaxin 4 (Stx4) has been suggested as endosomal interaction partner of Sec22b for mediating the fusion of ERGIC vesicles with the endosomal membrane, but experimental evidence for a role of Stx4 in cross-presentation is still pending.

In this study, we further explore the roles of Sec22b and Stx4 in the context of two candidate vaccine formulations that have the potential to cross-prime CTL responses, e.g. in cancer immunotherapy (1). First, poly(lactic-*co*-glycolic acid) (PLGA) microspheres (MS)

are among the most frequently explored polymer-based vaccine formulations due to their efficient uptake by APCs, their biodegradability, and overall safety (FDA approved since 1989) (15, 16). PLGA-MS show ideal properties to encapsulate protein, peptide, or cancer cell lysate-derived antigens (17, 18) and their potential to cross-prime antigen-specific CTLs responses after controlled and sustained release of their content has been demonstrated in various pre-clinical and clinical studies (15, 16). Second, synthetic long peptides (SLPs) are promising agents in vaccination, as they are safe, easy to administer and - compared to recombinant proteins - easier to produce (19, 20). By definition, SLPs are of 15–50 amino acids in length (21) and were shown to cross-prime CTL responses more efficiently than shorter peptide sequences that rather induced tolerance (22–24). Since vaccine formulations based on protein or peptide antigens require cross-presentation by APC to prime CTL responses, characterizing the intracellular pathways and molecular mechanisms involved in the related processes remains important to understand and further optimize current therapeutic strategies (25).

Previous studies have already elucidated important details about the cross-presentation pathways utilized by vaccine formulations based on PLGA-MS-encapsulated proteins (16, 26, 27) and SLPs (20, 22). As in both cases cross-presentation was shown to depend on a cytosolic pathway (21, 27–31), we were interested to evaluate the role of the SNARE proteins Sec22b and Stx4 in related processes. We therefore used CRISPR/Cas9-mediated genome editing to generate homozygous knockouts (KOs) of Sec22b and Stx4 in two established C57BL/6-derived APC cell lines and evaluated their effect on cross-presentation of the PLGA-MS-encapsulated model antigen ovalbumin (MS-OVA) and a related SLP (OVA-SLP). In contrast to previous findings, we did not observe an essential role of Sec22b in the cross-presentation of both antigen types in this system. In addition, we were - to our knowledge - the first to directly address the role of Stx4 in the context of cross-presentation. Similar to our findings with Sec22b KOs, we found no evidence for a major role of Stx4 KO in the cross-presentation of both MS-OVA and OVA-SLP under the conditions tested here. Overall, our study points towards SNARE protein redundancy in the cytosolic pathways of cross-presentation.

Material & Methods

Mice

C57BL/6J (H-2^b) mice were obtained from Charles River and kept under specific pathogen-free conditions during the experiments. C57BL/6-Tg(TcraTcrb)1100Mjb/Crl (OT-1) mice were initially obtained from Charles River and further maintained at the Erasmus MC animal facility under specific pathogen-free conditions. All experiments using *ex vivo* cell material were approved by the local authorities in the Netherlands (Centrale Commissie Dierproeven, license number AVD101002016793). Mice were sacrificed at 6–15 weeks of age.

Cell lines and culture media

The murine macrophage cell line BMC2 (H-2^b) (32) was originally obtained from K. Rock and cultured in RPMI 1640 (Gibco), supplemented with 25 mM HEPES. B3Z hybridoma

T-cells were a kind gift from N. Shastri (33) and were cultured in RPMI 1640 (Gibco). MutuDC2114 (MutuDC) dendritic cells were contributed by H. Acha-Orbea (34) and cultured in IMDM (Gibco), 35 mM HEPES (Gibco) and 50 μM β-mercaptoethanol (Life Technologies). HEK293T cells (ATCC, CRL-3216) were cultured in DMEM (Gibco). OT-1 T-cells were cultured in RPMI 1640 (Gibco), supplemented with 35 mM HEPES (Gibco), 2 mM L-glutamine (Lonza), 1 mM sodium pyruvate (Sigma), 1X non-essential amino acids (Gibco, 100x), 50 μM β-mercaptoethanol (Life Technologies). BMDCs were cultured in RPMI 1640 (Gibco), supplemented with 5 μM β-mercaptoethanol (Life Technologies) and 20 ng/ml recombinant mouse granulocyte macrophage colony stimulating factor (GM-CSF; PeproTech). All cell culture media were supplemented with 10% heat-inactivated FCS (Gibco) and 100 U/ml penicillin/streptomycin (Lonza). All cells were cultured at 37°C and in 5% CO_2. BMC2 and HEK293T cells were detached using 0.05% trypsin/EDTA (Gibco). MutuDCs and BMDCs were detached using 5 mM and 1mM EDTA/PBS (Merck), respectively.

Generation of bone marrow derived dendritic cells (BMDCs)

For preparation of BMDCs, femurs and tibias of C57BL6J mice were taken and their bone marrow isolated by crushing the bones in a mortar with PBS. Single cell suspensions were generated using a 70μm cell strainer and subsequently cultured in BMDC medium on non-cell culture treated petri dishes. Medium was refreshed after 4 days and cells were harvested for use in experiments after 7 days.

Generation of activated OT-1 T-cells

Splenocytes from OT-1 mice were obtained and mononuclear cells were isolated using Ficoll (Cytiva). Next, cells were stimulated with 10^{-8} M SIINFEKL peptide ($OVA_{257–264}$; Antibodychain) as well as 5 ng/ml of both mIL-7 and mIL-15 (PeproTech). On day five, live and dead cells were separated by using Ficoll. Remaining $CD8^+$ T-cells were allowed to rest in the presence of mIL-7 and mIL-15 for 48 hours before being used in the cross-presentation assays.

CRISPR/Cas9-mediated genome editing and lentivirus production

Single guide RNAs (sgRNAs) were designed using Benchling (an online platform for molecular biology design and analysis; benchling.com) and cloned into the LentiCRISPR.v2 plasmid (Addgene #52961) for all cell lines, except MutuDC/Stx4 KO, for which sgRNAs were cloned into lentiGuide-Puro (Addgene #52963). Sec22b sgRNAs targeting exon 1: sgRNA1 (5’-TGTGGCGGACGGCCTTCCGC-3’) and targeting exon 2: sgRNA2 (5’-GCTTCCAAGGTACATCGGGT-3’); STX4 sgRNAs targeting exon 2: sgRNA1 (5’-GGCGACAGGACCCACGAGTTG-3’) (BMC2 and MutuDC) and targeting exon 3: sgRNA2 for BMC2 (5’-GAGATGAGGTTCGAGTCGCGC-3’) and sgRNA2 for MutuDC (5’-GTGAGGTTCGAGTCGCGCTGG-3’). Non-targeting (NT) control sgRNAs are NT control 1 (5’-GCGAGGTATTCGGCTCCGCG-3’) and NT control 2 (5’-ATGTTGCAGTTCGGCTCGAT-3’), extracted from Sanjana *et al.*, 2014 (35). To clone the different sgRNAs, we annealed the forward oligo with the reverse, which were then ligated into the cut lentiviral backbone plasmid (lentiCRISPR.v2 or lentiGuide-Puro). First, both plasmids were cut using Esp3l (New England Biolabs) for 2h at 37°C, put on

agarose gel and purified from the gel (Qiaquick gel extraction kit, Qiagen) according to the manufacturer's instructions to obtain the linearized vector. Annealed oligos and cut vectors were then ligated using T4 DNA ligase according to the manufacturer's instructions (Life Technologies). Ligation reactions were transformed into homebrew-competent *E. Coli* (Stbl3, originally from Thermo Fisher, genotype: F^- *mcr*B *mrr*hsdS20(r_B^-, m_B^-) *rec*A13 *sup*E44 *ara*-14 *gal*K2 *lac*Y1 *pro*A2 *rps*L20(Str^R) *xyl*-5 λ^- *leumtl*-1). Transformation reactions were plated on LB-agar plates (Sigma) with 100 μg/ml ampicillin (Sigma) and incubated ON at 37°C. Single colonies were selected and grown in LB (Sigma) overnight with 100 μg/ml ampicillin. Plasmids were extracted by using a Qiaprep Spin miniprep kit (Qiagen) according to the manufacturer's instructions. Plasmids were checked for the correct insertion of the sgRNA by sanger sequencing at GATC Eurofins using the hU6 primer (5'-GACTATCATATGCTTACCGT-3'). To generate lentivirus containing the plasmids with either Sec22b or Stx4 KO sgRNAs, 6×10^5 HEK293T cells per well were seeded in a 6-well plate and grown to 70–80% confluency. The cells were then transfected with 500 ng packing plasmid (psPAX2, Addgene #12260) 50 ng envelope protein plasmid (pCMV-VSV-G, Addgene #8454) and 500 ng expression vector using Lipofectamine 2000 (Invitrogen), following the manufacturer's instructions. Lentivirus-containing supernatant was collected 24 hours and 48 hours post-transfection and filtered using a 0.2μm sterile filter to remove cell debris. To transduce BMC2 cells with Sec22b KO and Stx4 KO sgRNAs respectively, 6×10^5 cells per well were plated in a 6 well plate 18 hours before transduction. The next day, fresh medium containing 8 μg/mL polybrene (Sigma) and 500 μl of filtered lentivirus supernatant was added. The plates were then centrifuged at 2000 rpm for 90 minutes at 37°C. To transduce MutuDC with Sec22b KO sgRNAs, 5×10^6 cells were resuspended in 1 ml of lentivirus containing supernatant in the presence of 8 μg/ml polybrene, which was stirred every 30 min for 2 hours at 37°C. To target MutuDC with Stx4 KO sgRNAs, the cells were first targeted with a Cas9 expressing vector, lentiCas9-Blast (Addgene, #52962). This plasmid was delivered as a lentivirus, which was made in HEK293T cells as follows: HEK293T cells were plated as described above. Cells were transfected with 1000 ng packaging plasmid (psPAX2), 100 ng envelope protein plasmdid (pCMV-VSV-G) and 1000 ng of expression vector using TransIT VirusGEN (Mirus) following manufacturer's instructions. Supernatant containing lentivirus was collected after 48 hours and filtered as described above. MutuDC cells were transduced as described above with Sec22b KO sgRNAs and selected after three days using 5 μg/ml of blasticidin (InvivoGen). Monoclonal cultures were obtained by limited dilution, and Cas9 expression of monoclonal cell lines was confirmed on western blot (data not shown). MutuDC cells expressing Cas9 were then transduced with plasmids containing either Stx4 KO or non-targeting control sgRNAs in LentiGuide-Puro in lentivirus made as described above with TransIT VirusGEN. For all Sec22b and Stx4 KO cell lines: three days after transduction, APCs were selected using medium containing 6 μg/ml (BMC2) and 4 μg/ml (MutuDC) puromycin (Sigma). Monoclonal cultures were obtaining by limited dilution and clones were further characterized on genetic level using sanger sequencing and protein level by western blotting.

Validation of genome editing using Sanger sequencing

DNA was isolated from BMC2 and MutuDC cells using QIAamp DNA mini kit (Qiagen, 51306). Samples were amplified via PCR using Phusion High-Fidelity DNA polymerase (Life Technologies) according to the manufacturer's instructions. The following primers were used: Sec22b exon 1 FW: 5'-GGAGAAGAAGGGACAGTGA-3' and REV: 5'-ACGAGCAAACGGTAAAAGA-3', Sec22b exon 2 FW: 5'-GCTTTGTGTGATGTGTGTT-3' and REV: 5'-GCCCCTACTGTGATATTCTT-3', STX4 exon 2 and 3 FW: 5'-CACGACTGTGGATGGTGAAAGG-3' and REV: 5'-TAAGTGTCACTCTAGTCCGCCC-3'. PCR amplified products were loaded on agarose gels to check for a band at the expected size: 236 bp for Sec22b exon 1, 254 bp for Sec22b exon 2 and 536 bp for Stx4. PCR products were sent for sanger sequencing at GATC Eurofins using the forward and reverse primer, respectively. Results were aligned against the reference sequence of Sec22b (C57BL/6, ENSMUSG00000027879) or STX4 (C57BL/6, ENSMUSG00000030805) to evaluate cutting of the CRISPR/Cas9 machinery using the program CLC Workbench, version 7.

Western blotting

To confirm the absence of Sec22b or Stx4 protein in our KO cell lines, we lysed approx. 1×10^6 cells on ice using RIPA buffer (50 mM Tris-HCl, pH = 7.6; 150 mM NaCl; 1% NP-40; 0.5% sodium deoxychylate; 0.1% SDS; in H_2O), supplemented with Halt Protease and Phosphatase Inhibitor Cocktail (Thermo Fisher). Protein levels were determined using a Bradford protein assay (Sigma) and loaded on 4–15% polyacrylamide Tris-Glycine gels (Bio-Rad) that were run in Tris/Glycine/SDS (25 mM Tris, 192 mM Glycine, 0.1% SDS, pH = 8.3; Bio-Rad) buffer. After transfer of separated proteins to PVDF membranes using the Turbo-blot system (Bio-Rad), the membranes were blocked using 5% blocking grade non-fat milk (Bio-rad) in PBS containing 0.05 % of Tween-20 (Bio-Rad) (PBS-T) and incubated overnight at 4°C in PBS-T containing 2.5% blocking grade non-fat milk with primary antibodies (α-Sec22b, 1:400, mouse anti-mouse, SC101267, Santa Cruz; α-STX4, 1:3,000, rabbit anti-mouse, ab184545, Abcam; α-Actin, 1:3,000, rabbit anti-mouse, A2066, Sigma-Aldrich; α-β-Actin, 1:10,000, mouse anti-human, ab6276, Abcam). After washing using PBS-T, blots were incubated for 2 hours at room temperature with secondary antibodies (IRDYE-800CW, goat anti-mouse, 926–32210; IRDYE-680RD, goat anti-rabbit, 926–68071; Westburg BV; 1:7,500 dilution) in presence of PBS-T containing 2.5% blocking grade non-fat milk. After washing again with PBS-T, the fluorescent signal was measured with the Odyssey CLx Imaging System (Li-cor) and analyzed with Image Studio Lite version 5.2.5.

Preparation of PLGA particles

PLGA-MS were generated as previously described (26) with slight modifications. For antigen encapsulation, 50 mg ovalbumin (grade V, Merck) were dissolved in 1 ml of 0.1 M $NaHCO_3$ (aqueous phase) and emulsified with 1 g PLGA in 20 ml dichloromethane (organic phase) using a digital microtip sonicator. PLGA-MS labeled with fluorescent quantum dots (emission wavelength 583 nm; MS-QD) were generated by encapsulation of 50 mg ovalbumin as described above and by addition of QD583 into the dichloromethane phase

of the spray-drying process (27). The obtained dispersion was immediately spray-dried with the Mini Spray-Dryer 290 (Büchi Labortechnik AG) at a flow rate of 1 ml/min and inlet/outlet temperatures of 25 °C/23 °C. Spray-dried microspheres were washed out of the spray-dryer's cyclone with 0.05% Poloxamer 188 (Merck) and collected on a cellulose acetate membrane filter. PLGA-MS were dried under vacuum at room temperature and subsequently stored under desiccation at 4 °C. A fresh stock of MS-OVA or MS-QD was prepared for every experiment by weighing 4 mg MS-OVA and subsequent resuspension in APC medium to a concentration of 4 mg/ml. This suspension was sonicated for 1–2 minutes to ensure proper homogenization of MS-OVA.

Antigen uptake and cross-presentation assays

To evaluate the uptake of antigens, APCs were plated at 2.5×10^5 cells per well in a 24 well plate. APCs were incubated with 150 μg of MS-QD per well for 2 hours at either 37°C in medium or at 4°C in PBS supplemented with 0.5% BSA. APCs were detached and phagocytosis was evaluated using flow cytometry. To measure cross-presentation, APCs were plated in round-bottom 96-well plate (2.5×10^4 for 18-hour incubation (B3Z assay) and 1.0×10^5 APCs for 2-hour incubation (OT-1 T-cell assay)). Antigens ($OVA_{257–264}$ or SIINFEKL, S8L, Anaspec; OVA-SLP, $OVA_{252–271}$, LEQLESIINFEKLTEWTSSN, Genscript; PLGA-MS containing OVA, MS-OVA) were added at the indicated concentrations. For the inhibition assay, APCs were incubated for 30 min with either 100 μM leupeptin (Sigma), an inhibitor of cysteine, serine, and threonine proteases; 10 μM MG-132 (Merck), a proteasome inhibitor; or 10 μg/ml brefeldin A (Sigma) before adding indicated amounts of the antigens and incubating for an additional 2 hours. APCs were washed with PBS 2x before fixing with 1% PFA (diluted in PBS) for 10 min at 4°C. Cells were then washed 1x with PBS. Excess PFA was quenched by adding 0.2 M glycine for 5 min at RT. Hereafter, APCs were washed 3 times with PBS before adding 1.0×10^5 B3Z hybridoma cells. As a positive control and for peptide titration experiments to determine overall MHC class I surface expression, APCs were incubated for 1 hour with SIINFEKL and washed with PBS 3 times before adding 1.0×10^5 B3Z hybridoma cells. To determine cross-presentation after 18 hours of incubation with antigens, B3Z cells were added simultaneously to the wells. All conditions tested in the B3Z assays were performed in technical triplicates. For the 2-hour time points, APCs were incubated with antigen for 2 hours before adding 1.0×10^5 OT-1 T-cells per well in the medium of the APC cell line. OT-1 T-cells also received Protein Transport Inhibitor (1:1,000, BD) and the assay was incubated for 4 hours at 37°C. All conditions tested in the OT-1 assays were performed in technical duplicates. Afterwards OT-1 T-cell activation was quantified by intracellular cytokine staining for IFN-γ using flow cytometry. After 18 hours incubation with APCs and B3Z hybridomas, cells were washed once with PBS and chlorophenol red-β-D-galactopyranoside (CPRG) (59767, Sigma) substrate in a PBS buffer containing 0.13% IGEPAL (Sigma) and 9 mM $MgCl_2$ (Merck) was added to detect β-galactosidase activity as a measure of T cell activation. Substrate conversion was measured at an optical density (OD) of 570nm and a control at OD 620nm on a VersaMax ELISA microplate reader. The final OD was calculated by subtracting the values at 620 nm from those at 570nm. Plate was measured every 30–60 min until the positive control condition (10^{-6} M SIINFEKL) reached a calculated OD of 1.0. For the inhibition assay, values were normalized to the control

condition, which was APCs plus antigen without inhibitors, showing the highest amount of cross-presentation possible for BMC2, MutuDC or BMDC with the respective antigen (MS-OVA or OVA-SLP). Control conditions were then normalized to their respective means.

Fluorescence stainings and flow cytometry

To investigate the expression levels of H-2K^b and H-2D^b on APCs, the cells were detached, washed to remove all serum, and resuspended in FACS buffer containing 0.5% BSA and 0.1% sodium azide. Next, they were stained in presence of FACS buffer for 30 min on ice (α-H2Db-PE, 1:200, mouse anti-mouse, 12–5999-81; α-H2Kb-PE, 1:200, 12–5958-80; Life Technologies). Hereafter cells were washed with a surplus of FACS buffer to remove excess antibody. Samples were gated on live cells using FSC/SSC, followed by singlet gating using FSC-A and FSC-H. To measure the activation of OT-1 T-cells by intracellular cytokine staining of IFN-γ, the T-cells were stained extracellularly for 20 min at 4°C in FACS buffer (α-CD8a-eF450, 1:80, Thermo Fisher, 48–0081-82), washed twice with FACS buffer and fixed using IC Fixation buffer (Thermo Fisher, 00–8833-56). T-cells were then washed once with permeabilization buffer (Thermo Fisher, 00–8222-49) and stained intracellularly in presence of permeabilization buffer for 45 min at 4°C (α-IFN-γ-APC, 1:160, Thermo Fisher, 17–7311-82). Samples were washed once with permeabilization buffer, once with FACS buffer and then resuspended in FACS buffer for subsequent measurements. One technical replicate was used per experiment. Live T-cells were gated on FSC/SSC, then on singlets using FSC-A and FSC-H, followed by CD8 gating using CD8$^+$ and SSC, and finally, IFN-γ+ cells were gated on CD8+ and IFN-γ+ (for all gating strategy see Suppl Fig. 2). All samples were run on the CANTO II (BD) and analyzed using FlowJo (version 10; BD Life Sciences).

Quantification and statistical analysis

Unless otherwise stated, data are shown as the mean ± standard deviation (SD). Unless indicated otherwise, the median fluorescence intensity (MFI) of flow cytometry data was used for quantification. Statistical analyses of results were done using Graphpad PRISM v9. Methods for statistical testing are listed in the respective figure legends.

Results

Cross-presentation of MS-OVA and OVA-SLP mainly follows a cytosolic pathway

In order to investigate the role of Sec22b and Stx4 in the cross-presentation of PLGA-MS-encapsulated antigens and SLPs, we decided to select two murine APC lines; the macrophage cell line BMC2 (32) and the CD8$^+$ dendritic cell line MutuDC (34). Both cell lines have previously been used to explore the mechanisms of cross-presentation (32, 34, 36–39), and they efficiently cross-present the H-2K^b-restricted, chicken ovalbumin (OVA)-derived epitope SIINFEKL (S8L, OVA$_{257–264}$) after incubation with PLGA-MS-containing full-length OVA (MS-OVA) or a S8L-containing 20-mer SLP (OVA$_{252–271}$; OVA-SLP). As Sec22b has previously been assigned a role in the cytosolic pathway of cross-presentation, we initially evaluated which intracellular pathways were utilized for the cross-presentation of MS-OVA and OVA-SLP by the APC lines selected for this study. We therefore studied cross-presentation of MS-OVA and OVA-SLP in the presence of specific inhibitors that

interfere with key steps of antigen processing and intracellular transport (Fig. 1a). To allow time for the inhibitors to act before adding the antigens, we pre-incubated APC lines with the compounds for 30 min, before adding the two different OVA-based antigens, respectively (Fig. 1b). After two hours of incubation, APCs were fixed and co-cultured with the S8L-specific T-cell hybridoma cell line B3Z (33), using T-cell activation as a measure for cross-presentation efficiency. These experiments revealed that cross-presentation of MS-OVA and OVA-SLP by BMC2 macrophages was sensitive to the reversible proteasome inhibitor MG-132 (40, 41) and the secretory pathway inhibitor Brefeldin A (BFA) (36, 42) (Fig. 1c), with the interesting observation that cross-presentation of OVA-SLP was preferentially inhibited by interfering with proteasomal activity. In contrast, treatment with leupeptin, an inhibitor of cysteine, serine, and threonine proteases important for endosomal processing (36, 43–45), did not affect the cross-presentation efficiency detected for both antigens tested. We therefore concluded that MS-OVA and OVA-SLP follow the cytosolic pathway of cross-presentation in BMC2 cells. Also in case of MutuDC cells, cross-presentation of the same antigens was sensitive to MG132 and BFA, but not to leupeptin, again indicating a dependency on the cytosolic pathway (Fig. 1d). Similar results were obtained when performing the same experiment with primary wildtype bone marrow-derived dendritic cells (BMDCs; Suppl. Fig. 1). Overall, it was therefore evident that presentation of MS-OVA and OVA-SLP by both APC lines largely depended on the cytosolic pathways of cross-presentation. We therefore considered our experimental setup as a valid model to study the role of Sec22b and Stx4 in the cross-presentation of these antigens.

Sec22b knockout does not alter normal surface expression of MHC class I

To investigate the role of Sec22b in the cross-presentation of MS-OVA and OVA-SLP, we used CRISPR/Cas9-mediated genome editing to generate homozygous knockout (KO) clones for both BMC2 and MutuDC cells. To reduce the risk of potential off-target effects in our experiments, we targeted both exon 1 and 2 of Sec22b, respectively, with two different, non-homologous single guide RNAs (sgRNAs) (Fig. 2a). We thereby generated two independent Sec22b KO clones for both APC lines that we aimed to use for our cross-presentation experiments. As controls, we transduced wildtype APCs with non-targeting sgRNAs to ensure that the experimental procedure of generating Sec22b KO clones had no additional Sec22b-independent effects on the phenotype of APCs. After lentiviral targeting of APCs, single cell clones (Sec22b KOs) or non-targeting pools of cells (controls) were tested by western blot analysis to evaluate Sec22b expression. This experiment revealed that while both BMC2 (Fig. 2b) and MutuDC cells (Fig. 2c) showed prominent expression of Sec22b for wildtype and non-targeting controls at the expected size of ~24 kDa, this expression was completely absent in single-cell clones targeted with Sec22b-specific sgRNAs. These results demonstrated that we successfully generated two independent Sec22b KO clones for both BMC2 and MutuDC cells, respectively.

As functional MHC class I surface expression is an important parameter for evaluation of cross-presentation efficiency, we next wanted to ensure that Sec22b KO did not affect the overall amount of MHC class I surface expression of targeted APCs. For this purpose, we stained the cells with fluorescently-labeled antibodies against the two C57BL/6-specific MHC class I alleles H-2K^{b} and H-2D^{b} and analyzed their surface expression by flow

cytometry (Fig. 2d+e, Suppl. Fig. 2a–c). Of note, we did not observe any alteration of MHC class I expression when comparing wildtype APCs with cells that were modified with non-targeting control sgRNAs, demonstrating that introducing the CRISPR/Cas9 machinery alone had no effect on MHC class I surface levels. Although both Sec22b KO clones of BMC2 cells (Fig. 2d) and one clone of MutuDC (Fig. 2e) showed a small reduction in the overall H-2K^b surface expression, this phenotype was not significant. In support of this notion, we also did not observe a significant reduction of H-2D^b expression that was monitored in parallel (Suppl. Fig. 2b+c).

To independently validate these results, we used B3Z T-cell hybridoma activation as a functional readout to quantify the overall MHC class I-restricted antigen presentation capacity by Sec22b KO cells and non-targeting controls (Fig. 2f+g). APCs were externally pulsed with titrated amounts of the minimal peptide epitope S8L that binds to surface H-2K^b without requiring internalization and further processing. After removing unbound peptides, pulsed cells were co-cultured with B3Z T-cell hybridoma cells overnight. When comparing Sec22b KO clones with the non-targeting controls, we observed no differences in B3Z activation for BMC2 cells line. Similar, for MutuDCs – and despite a slight but significant reduction observed for KO clone 1 - Sec22b KO did overall not affect the celĺs capacity to activate B3Z hybridomas. We therefore decided to continue with both BMC2 and MutuDC clones to evaluate possible effects of Sec22b KO on the cross-presentation of MS-OVA and OVA-SLP.

APCs lacking Sec22b efficiently cross-present MS-OVA and OVA-SLP

Before investigating the role of Sec22b in cross-presentation, we evaluated antigen uptake as a critical first step of the cross-presentation pathway. PLGA-MS containing fluorescent quantum dots (MS-QD) were used to evaluate the phagocytic abilities of Sec22b KO APCs. Cells were incubated with MS-QD for two hours before samples were analyzed by flow cytometry. This experiment showed that equal amounts of MS-QD were phagocytosed by BMC2 cells, when comparing Sec22b KO clones with either non-targeting controls or wildtype cells (Fig. 3a). The same assay performed at 4°C showed strongly reduced fluorescence signals, indicating that MS-QD uptake by APCs depended on an active cellular process, as expected. While BMC2 cells lacking Sec22b showed unaltered levels of phagocytosis, it appeared that Sec22b KO in MutuDCs lead to a slight reduction in the overall phagocytosis capacity (Fig. 3b).

As a next step, we evaluated the effect of Sec22b KO on the cross-presentation of MS-OVA and OVA-SLP using two different T-cell assays as readout for the quantification of H-2K^b/S8L surface presentation. First, we tested the cross-presentation efficiency of BMC2 using primary H-2K^b/S8L-restriced T-cells from T-cell receptor transgenic OT-1 mice as a readout. In the light of recent studies that showed an effect of Sec22b-deficiency on the cross-presentation of different OVA-derived antigens (9, 13, 14), we used a similar experimental setup with restricted time for antigen processing and presentation. BMC2 cells were incubated with antigen for two hours before co-incubation with OT-1 T-cells for additional four hours in the presence of BFA. Next, the percentage of interferon (IFN)-γ-positive CD8$^+$ T-cells was quantified by flow cytometry as a measure of T-cell activation.

Interestingly, in BMC2 cells Sec22b KO had no consistent effect on the cross-presentation efficiency observed for both MS-OVA and OVA-SLP, compared to the non-targeting controls (Fig. 3c, top panels). To independently validate these finding, we repeated our experiments using the B3Z hybridoma assay. In this setting, wildtype and Sec22b KO APCs were incubated with antigen and simultaneously co-cultured with B3Z hybridoma cells for 18 hours. Again, these experiments revealed that overall Sec22b KO did not interfere with cross-presentation of both antigens (Fig. 3c, bottom panels).

To further investigate the role of Sec22b in the cross-presentation of MS-OVA and OVA-SLP, we performed the same set of experiments with MutuDC cells (Fig. 3d). Similar to our experiments with BMC2 cells, we did not observe a consistent reduction in the cross-presentation capacity of Sec22b KO MutuDC cells when incubating with MS-OVA or OVA-SLP for 2 hours followed by addition of primary OT-1 T-cell. Although, Sec22b KO clone 1 consistently showed reduced cross-presentation of MS-OVA, this effect appeared to be unrelated to Sec22b expression, as the independently generated KO clone 2 was able to cross-present normally (Fig. 3d, top panels). The small reduction seen for overall H-2K^{b} expression of KO clone 1 may explain this reduction (Fig. 2g). Next, we again wanted to independently validate these results by co-incubating Sec22b KO MutuDC cells with antigen and B3Z T-cell hybridoma cells for 18 hours. This assay showed robust cross-presentation of both MS-OVA and OVA-SLP that was not consistently different compared to the non-targeting controls (Fig. 3d, bottom panels). Interestingly, cross-presentation of MS-OVA rather seemed slightly increased in Sec22b KO MutuDCs. Together, we did not observe a consistent cross-presentation-related phenotype in Sec22b KO APCs under the conditions tested in this study.

Stx4 knockout does not affect MHC class I surface expression on both BMC2 and MutuDC cells

In recent literature, Sec22b has been suggested to mediate membrane fusion events in collaboration with the t-SNARE syntaxin 4 (Stx4) (4, 9, 46). For the cytosolic pathways of cross-presentation, however, experimental data regarding a functional role of Stx4 is still pending. In this study, we therefore aimed to experimentally evaluate the role of Stx4 in the context of antigen cross-presentation. Using a similar CRISPR/Cas9-mediated genome editing strategy as used to make the Sec22b KO APC clones, we generated two independent homozygous Sxt4 KO clones for the two APC cell lines BMC2 and MutuDC. Again, two non-homologous sgRNAs were designed that targeted exon 2 and exon 3 of Stx4, respectively (Fig. 4a). After introducing the CRISPR/Cas9 machinery and the sgRNAs using a lentiviral approach, successfully targeted cells were selected by puromycin or blasticidin resistance, and APCs were subcloned to obtain single cell clones. Next, the targeted cells were evaluated by western blot analysis for their Stx4 protein expression (Fig. 4b+c). While both wildtype BMC2 and MutuDC cells, as well as respective controls targeted with two different non-targeting sgRNAs, showed a prominent Stx4-specific band at the expected molecular weight of 34 kDa, no residual expression of Stx4 was observed in APC clones targeted with Stx4-specific sgRNAs. We therefore concluded that we successfully generated viable Stx4 KO clones of both BMC2 and MutuDC cells, which allowed us to study the role of Stx4 in the cross-presentation of MS-OVA and OVA-SLP.

We next evaluated possible effects of Stx4 KO on the overall surface expression of MHC class I, as a prerequisite for antigen cross-presentation. APCs were stained for H-2K^b and H-2D^b, respectively, and analyzed by flow cytometry (Fig. 4d+e, Suppl. Fig. 3). This experiment demonstrated that Stx4 KO did not alter MHC class I surface expressing on both APC cell lines tested. Although there was a slight trend towards reduced H-2K^b and H-2D^b surface expression levels in BMC2 cells targeted with Stx4 KO sgRNA 1 and 2, these differences were not significant. To independently validate these results, we again used T-cell activation as a second readout to evaluate surface H-2K^b expression. Therefore, APCs were externally pulsed with titrated amounts of the minimal T-cell epitope S8L, followed by washing steps to remove unbound peptide and incubation with B3Z hybridoma cells. Similar to the initial characterization of Sec22b KO clones (Fig. 2f+g), we did not detect major differences between Stx4 KO BMC2 clones and non-targeting controls (Fig. 4f). The Stx4 KO clones in MutuDC cells were similar to the non-targeting controls, although a small reduction was observed for the limiting peptide concentrations that was consistent for both KO clones (Fig. 4g). Next, we continued to evaluate the role of Stx4 in the cross-presentation of MS-OVA and OVA-SLP in the following experiments.

Stx4 knockout has no major effect on cross-presentation of OVA-SLP and MS-OVA

Similar to the characterization of Sec22b KO APCs, we initially investigated antigen uptake by Stx4 KO clones as a first, essential requirement for cross-presentation. Wildtype, non-targeting control, and Stx4 KO APCs were incubated with fluorescent MS-QD for two hours and uptake efficiency was quantified by flow cytometry (Fig. 5a+b). The results of these experiments revealed that Stx4 KO did not alter the capacity to efficiently take up MS-QDs in both BMC2 (Fig. 5a) and MutuDC cells (Fig. 5b). The fluorescence intensity after incubating APCs at 4°C was strongly reduced, indicating that the MS-QD-specific signal was based on active endocytosis.

Next, we evaluated the effect of Stx4 KO on the cross-presentation of MS-OVA and OVA-SLP in both APC cell lines, using primary OT-1 T-cell activation and B3Z hybridoma as a measure of cross-presentation efficiency. Initially, BMC2 cells were incubated for two hours with antigen, before OT-1 T-cells were added for additional 4 hours (Fig. 5c, top panels). These experiments revealed that cross-presentation of both MS-OVA and OVA-SLP was not compromised by Stx4 KO BMC2 cells. We next aimed to validate these findings using the B3Z hybridoma assay as an independent readout for cross-presentation (Fig. 5c, bottom panels). For these experiments, BMC2 cells and B3Z hybridoma cells were co-cultured for 18 hours in the presence or absence of MS-OVA or OVA-SLP. Interestingly, while cross-presentation of OVA-SLP was not consistently affected by Stx4 KO (Fig. 5c, bottom right panel), the activation of B3Z hybridomas after incubation with MS-OVA was significantly reduced in both Stx4 KO clones (Fig. 5c, bottom left panel). Therefore, although we did not observe this in the OT-1 T-cell assay, it appears that under specific experimental conditions (antigen type, time of incubation, readouts system) Stx4 might play a non-redundant role in cross-presentation.

Next, we evaluated the effects of Stx4 KO on the cross-presentation of MS-OVA and OVA-SLP in MutuDC cells, using the same set of experiments. Of note, we did not observe

any reduction in T-cell activation (OT-1 T-cell and B3Z hybridoma assay), indicating that cross-presentation was not affected by Stx4 KO in any of the conditions tested (Fig. 5d). This led us to the conclusion that Stx4-depletion in the two APC lines tested had overall very limited effect on the cross-presentation of MS-OVA and OVA-SLP.

Discussion

The contribution of specific SNARE proteins to cross-presentation is an ongoing subject of discussion (9, 13, 14, 47), and we therefore set out to specifically investigate the role of Sec22b and Stx4 in related pathways. Initially, we confirmed dependence of MS-OVA and OVA-SLP cross-presentation by BMC2 macrophages and MutuDCs on the cytosolic pathway, which was an important validation of previous findings (21, 27–31) and essential to qualify our experimental setup. Of note, both APC lines have been used as model systems reflecting aspects of *in vivo*-relevant mechanisms of cross-presentation (32, 34, 36–39). Still, our experiments point towards cell line and antigen-specific pathway preferences, as the inhibitory effect of MG-132 on OVA-SLP presentation seemed more pronounced in BMC2 cells compared to MutuDCs. This was accompanied by a remarkably reduced effect of Brefeldin A treatment under the same condition, indicating that cross-presentation of OVA-SLP in BMC2 cells but not MutuDCs might have primarily relied on the indirect cytosolic pathways (P2C2P) (3, 4, 6). When comparing the cross-presentation efficiency of MS-OVA in the presence of MG132 and Brefeldin A between BMC2 cells and MutuDCs, it was evident that both inhibitors lead to a comparable reduction, arguing for a contribution of the direct cytosolic pathway (P2C) in this system (6). Though DCs are generally considered the most relevant cross-presenting cell type *in vivo* (3), especially for cell-associated antigens, macrophages can process and cross-present exogenous antigen delivered by vaccines formulations (48, 49). For example, cross-priming of $CD8^+$ T-cells of MS-OVA was only compromised after depleting both dendritic cells and macrophages *in vivo* (26). In addition, a similar dependence on the cytosolic pathways was also observed when performing the same experiments with primary bone marrow-derived dendritic cells (BMDCs), indicating that this was not specific for the cell lines selected for this study (Suppl. Fig. 1a+b). Of note, some PLGA-based polymers have previously been described to grant encapsulated antigens artificial access to the direct MHC class I presentation pathway by inducing endosomal membrane rupture (31, 50). However, for the MS-OVA formulation used in our study, this mechanism has previously been excluded (27).

The v-SNARE protein Sec22b has been found on the ERGIC as well as on phagosomal/endosomal membranes, positioning it at the right place for mediating membrane fusion events between the ERGIC and antigen-containing endosomes (9, 51–53). For these reasons, the role of Sec22b in cross-presentation has been investigated before by Cebrian *et al.* (9). Using small hairpin RNAs (shRNAs) targeting Sec22b mRNA, this study reported that knockdown of Sec22b protein *in vitro* decreased the cross-presentation efficiency of different types of ovalbumin-based antigens, a finding that has been confirmed by another study (9, 12). Additionally, two groups have separately generated a conditional KO mouse for Sec22b in DCs via the use of Cre-expression under control of the CD11c promoter (13, 14). Alloatti *et al.* showed *ex vivo* and *in vivo* that Sec22b expression was essential for efficient cross-presentation of various OVA-based model antigens (13). Conversely, a

similar conditional Sec22b KO model generated by Wu *et al.* showed no defect in cross-presentation as tested *ex vivo* (14). A critical factor in both models might have been variable residual Sec22b expression, on either a cellular (shRNA approach) or a population level (conditional KO) (13, 14, 47). In contrast to previous studies, we therefore made use of CRISPR/Cas9-mediated genome editing technology to generate homozygous KOs for Sec22b and Stx4, respectively, which allowed us for the first time to study cross-presentation in complete absence of residual protein expression. To circumvent possible off-target effects that were discussed as confounding factors in some of the above studies (14), we used two distinct sgRNAs targeting both Sec22b and Stx4 in different exons, respectively. Using this model, we showed that Sec22b depletion had no consistent effect on the cross-presentation of MS-OVA and OVA-SLP in this system, which was in line with similar experiments performed by Wu *et al.* (14), but in contrast to earlier findings by Cebrian and Alloatti *et al.* (9, 13). Importantly, our results do not exclude a redundant role of Sec22b in the delivery of ER proteins to the endosome that might depend on the type and concentration of antigen as well as cell-type-specific factors and the time allowed for antigen processing that might determine pathway vulnerabilities. In both cases, other v-SNARE proteins might have rescued the cross-presentation-related phenotype of Sec22b KO APCs, as a certain degree of redundancy has been reported among SNARE proteins of the same family (54–56). This has particularly been demonstrated for Sec22b and its yeast homolog Sec22p (56, 57). The SNARE protein Ykt6p has been shown to substitute for Sec22p in the early secretory pathway in yeast (57). It is therefore possible that the murine homolog Ykt6 might replace Sec22b to promote the delivery of ER resident proteins to antigens-containing endosomes. However, Ykt6 could not be detected in phagosomes from both wildtype and Sec22b knockdown BMDCs containing latex beads (9), but this might be different for phagosomes containing MS-OVA or OVA-SLP. Other SNARE proteins that could possibly take over a Sec22b-related function include Vamp2, which has been demonstrated to be interchangeable with Sec22b in biochemical interaction studies (58). For future studies, it would therefore be interesting to study Sec22b KO APCs lacking additional SNARE proteins to evaluate possible redundancies in antigen cross-presentation.

The SNARE protein Stx4 is commonly found on the plasma membrane of cells where it mediates vesicle fusion events (9, 11, 56, 59–61). In DCs however, Stx4 is also present on early phagosomes where it interacts with Sec22b, most likely travelling along during the uptake of antigens (9, 46). Although frequently associated with vesicle fusion (11), to our knowledge the role of Stx4 in the cross-presentation of any type of antigen has never been addressed experimentally; making our study the first to explore possible effects of Stx4 KO on cross-presentation. In contrast to previous findings using an shRNA approach to deplete Stx4, the KO clones generated in this study were viable and did not show any obvious phenotype compared to wildtype APCs (9). When analyzing the consequences of Stx4 KO on cross-presentation we observed no major phenotype in both BMC2 and MutuDC cells, as both MS-OVA and OVA-SLP were cross-presented with at least the efficiency of the non-targeting controls. Reduced cross-presentation that we observed for MS-OVA in Stx4 KO BMC2 cells using the B3Z hybridoma assay was not evident when using primary OT-1 T-cells as a readout. Since MS-OVA uptake and related cross-presentation pathway dependencies observed in our inhibitor experiments were similar between BMC2 cells and

MutuDCs (Fig. 3a+5a; Fig. 1c+d), the different T-cell readouts might have accounted for the varying effects of the Stx4 KO in this condition. While both restricted to H-2K^b/S8L, B3Z hybridoma activation requires long co-incubation (18h) with APCs to accumulate beta-galactosidase, possibly integrating differences in cross-presentation that might occur late after antigen uptake. Activation of OT-1 T-cells in contrast is measured shortly (4h) after co-incubation with APCs, therefore representing a snapshot of the initial hours of cross-presentation. Given their primary origin, OT-1 T-cells might in addition require less MHC/peptide complexes per APC for full activation, which could also explain the overall stronger activation of OT-1 T-cells already at lower antigen concentrations. At the same time, this effect could have favored B3Z hybridomas in our setup to trace subtle effects of Stx4 KO in MS-OVA-treated BMC2 cells.

Overall, our results argue against a major role of Stx4 in the cross-presentation settings tested in this study, indicating the presence of alternative mechanisms and/or compensatory mechanisms (e.g. SNARE protein redundancy, alternative pathways) that might have rescued cross-presentation in Stx4 KO APCs. Possible redundancies of Stx4 with other SNARE proteins might be supported by indirect evidence suggesting that Stx4, together with SNAP-23, can interact with several other SNARE proteins including VAMP2, VAMP4, VAMP7 and VAMP8 (58, 59, 61). Additionally, Stx5 was reported to interact with Sec22b in the context of ER-to-Golgi trafficking, but could not directly been linked to cross-presentation, as Stx5 knockdown reduced steady state surface MHC class I expression and interfered with T-cell activation (9). Similar, Sec22b/Stx18 interactions were shown to regulate phagocytosis by macrophages, but a connection to ERGIC trafficking during cross-presentation has not been established (51, 52). Further investigating the network of specific SNARE proteins involved in cross-presentation therefore remains important to fully elucidate possible redundancies present in this pathway.

In this study, we did not find evidence for a role of Sec22b and Stx4 in most of the experimental conditions tested, highlighting that the previously suggested model of Sec22b/Stx4 function might not fully reflect the complexity of cross-presentation mechanisms present in the various types of APCs and with different antigens. The results of this study lead us to three general conclusions: a) SNARE proteins involved in the cytosolic pathways of cross-presentation might be redundant, b) the molecular machinery of cross-presentation – including the selection of specific SNARE proteins involved – may vary by APC and antigen type or concentration/time after uptake, and c) other compensatory mechanisms in the absence of specific SNARE proteins (e.g. use of alternative pathways) might further complicate experimental interpretations. Furthermore, we cannot exclude the presence of compensatory effects as a direct consequence of SNARE protein-depletion in our system that would not be present in the wildtype situation. Overall, our study adds to the current discussion about the role of SNARE proteins in the cytosolic pathways of cross-presentation and highlights the need of a differentiated, cell and antigen type-specific evaluation of the mechanisms involved. In addition, our results contribute to a better understanding of the cell-biological mechanisms involved in the cross-presentation of PLGA-MS and SLP-based antigen delivery systems, which might eventually help to further improve their potential to elicit potent and lasting CTL response in cancer vaccination.

Supplementary Material

Refer to Web version on PubMed Central for supplementary material.

Acknowledgements

We thank Marcus Groettrup for providing PLGA microspheres containing the model antigen ovalbumin, Manzhi Zhao and Ling Li for advice and technical support, and Peter D. Katsikis for critical input and helpful suggestions for this manuscript. Finally, we express our gratitude to the Department of Immunology at the Erasmus MC for generous financial support and research space.

This project was supported by the Department of Immunology at the Erasmus MC, a PhD fellowship from the Chinese Scholarship Council (CSC) to Z. Song, a LEaDing Postdoc fellowship to G. Mishra (a Horizon 2020 Marie-Skłodowska-Curie COFUND), and a National Institutes of Health (NIH) R21 grant (CA274064) to C. Schliehe.

References

1. Hu Z, Ott PA, and Wu CJ. 2018. Towards personalized, tumour-specific, therapeutic vaccines for cancer. Nat Rev Immunol 18: 168–182. [PubMed: 29226910]
2. Rock KL, Reits E, and Neefjes J. 2016. Present Yourself! By MHC Class I and MHC Class II Molecules. Trends Immunol 37: 724–737. [PubMed: 27614798]
3. Joffre OP, Segura E, Savina A, and Amigorena S. 2012. Cross-presentation by dendritic cells. Nat Rev Immunol 12: 557–569. [PubMed: 22790179]
4. Embgenbroich M, and Burgdorf S. 2018. Current Concepts of Antigen Cross-Presentation. Front Immunol 9: 1643. [PubMed: 30061897]
5. Pulendran B, P SA, and O'Hagan DT. 2021. Emerging concepts in the science of vaccine adjuvants. Nat Rev Drug Discov 20: 454–475. [PubMed: 33824489]
6. Colbert JD, Cruz FM, and Rock KL. 2020. Cross-presentation of exogenous antigens on MHC I molecules. Curr Opin Immunol 64: 1–8. [PubMed: 31927332]
7. Ackerman AL, Giodini A, and Cresswell P. 2006. A role for the endoplasmic reticulum protein retrotranslocation machinery during crosspresentation by dendritic cells. Immunity 25: 607–617. [PubMed: 17027300]
8. Imai J, Hasegawa H, Maruya M, Koyasu S, and Yahara I. 2005. Exogenous antigens are processed through the endoplasmic reticulum-associated degradation (ERAD) in cross-presentation by dendritic cells. Int Immunol 17: 45–53. [PubMed: 15546887]
9. Cebrian I, Visentin G, Blanchard N, Jouve M, Bobard A, Moita C, Enninga J, Moita LF, Amigorena S, and Savina A. 2011. Sec22b regulates phagosomal maturation and antigen crosspresentation by dendritic cells. Cell 147: 1355–1368. [PubMed: 22153078]
10. Nair-Gupta P, Baccarini A, Tung N, Seyffer F, Florey O, Huang Y, Banerjee M, Overholtzer M, Roche PA, Tampe R, Brown BD, Amsen D, Whiteheart SW, and Blander JM. 2014. TLR signals induce phagosomal MHC-I delivery from the endosomal recycling compartment to allow cross-presentation. Cell 158: 506–521. [PubMed: 25083866]
11. Malsam J, Kreye S, and Sollner TH. 2008. Membrane fusion: SNAREs and regulation. Cell Mol Life Sci 65: 2814–2832. [PubMed: 18726177]
12. Barbet G, Nair-Gupta P, Schotsaert M, Yeung ST, Moretti J, Seyffer F, Metreveli G, Gardner T, Choi A, Tortorella D, Tampe R, Khanna KM, Garcia-Sastre A, and Blander JM. 2021. TAP dysfunction in dendritic cells enables noncanonical cross-presentation for T cell priming. Nat Immunol 22: 497–509. [PubMed: 33790474]
13. Alloatti A, Rookhuizen DC, Joannas L, Carpier JM, Iborra S, Magalhaes JG, Yatim N, Kozik P, Sancho D, Albert ML, and Amigorena S. 2017. Critical role for Sec22b-dependent antigen cross-presentation in antitumor immunity. J Exp Med 214: 2231–2241. [PubMed: 28663435]
14. Wu SJ, Niknafs YS, Kim SH, Oravecz-Wilson K, Zajac C, Toubai T, Sun Y, Prasad J, Peltier D, Fujiwara H, Hedig I, Mathewson ND, Khoriaty R, Ginsburg D, and Reddy P. 2017. A Critical

Analysis of the Role of SNARE Protein SEC22B in Antigen Cross-Presentation. Cell Rep 19: 2645–2656. [PubMed: 28658614]

15. Park K, Skidmore S, Hadar J, Garner J, Park H, Otte A, Soh BK, Yoon G, Yu D, Yun Y, Lee BK, Jiang X, and Wang Y. 2019. Injectable, long-acting PLGA formulations: Analyzing PLGA and understanding microparticle formation. J Control Release 304: 125–134. [PubMed: 31071374]
16. Koerner J, Horvath D, and Groettrup M. 2019. Harnessing Dendritic Cells for Poly (D,L-lactide-co-glycolide) Microspheres (PLGA MS)-Mediated Anti-tumor Therapy. Front Immunol 10: 707. [PubMed: 31024545]
17. Mueller M, Reichardt W, Koerner J, and Groettrup M. 2012. Coencapsulation of tumor lysate and CpG-ODN in PLGA-microspheres enables successful immunotherapy of prostate carcinoma in TRAMP mice. J Control Release 162: 159–166. [PubMed: 22709589]
18. Schlosser E, Mueller M, Fischer S, Basta S, Busch DH, Gander B, and Groettrup M. 2008. TLR ligands and antigen need to be coencapsulated into the same biodegradable microsphere for the generation of potent cytotoxic T lymphocyte responses. Vaccine 26: 1626–1637. [PubMed: 18295941]
19. Supabphol S, Li L, Goedegebuure SP, and Gillanders WE. 2021. Neoantigen vaccine platforms in clinical development: understanding the future of personalized immunotherapy. Expert Opin Investig Drugs 30: 529–541.
20. Chen X, Yang J, Wang L, and Liu B. 2020. Personalized neoantigen vaccination with synthetic long peptides: recent advances and future perspectives. Theranostics 10: 6011–6023. [PubMed: 32483434]
21. Menager J, Ebstein F, Oger R, Hulin P, Nedellec S, Duverger E, Lehmann A, Kloetzel PM, Jotereau F, and Guilloux Y. 2014. Cross-presentation of synthetic long peptides by human dendritic cells: a process dependent on ERAD component p97/VCP but Not sec61 and/or Derlin-1. PLoS One 9: e89897. [PubMed: 24587108]
22. Bijker MS, van den Eeden SJ, Franken KL, Melief CJ, van der Burg SH, and Offringa R. 2008. Superior induction of anti-tumor CTL immunity by extended peptide vaccines involves prolonged, DC-focused antigen presentation. Eur J Immunol 38: 1033–1042. [PubMed: 18350546]
23. Toes RE, Blom RJ, Offringa R, Kast WM, and Melief CJ. 1996. Enhanced tumor outgrowth after peptide vaccination. Functional deletion of tumor-specific CTL induced by peptide vaccination can lead to the inability to reject tumors. J Immunol 156: 3911–3918. [PubMed: 8621930]
24. Rosalia RA, Quakkelaar ED, Redeker A, Khan S, Camps M, Drijfhout JW, Silva AL, Jiskoot W, van Hall T, van Veelen PA, Janssen G, Franken K, Cruz LJ, Tromp A, Oostendorp J, van der Burg SH, Ossendorp F, and Melief CJ. 2013. Dendritic cells process synthetic long peptides better than whole protein, improving antigen presentation and T-cell activation. Eur J Immunol 43: 2554–2565. [PubMed: 23836147]
25. Fehres CM, Unger WW, Garcia-Vallejo JJ, and van Kooyk Y. 2014. Understanding the biology of antigen cross-presentation for the design of vaccines against cancer. Front Immunol 5: 149. [PubMed: 24782858]
26. Schliehe C, Redaelli C, Engelhardt S, Fehlings M, Mueller M, van Rooijen N, Thiry M, Hildner K, Weller H, and Groettrup M. 2011. CD8- dendritic cells and macrophages cross-present poly(D,L-lactate-co-glycolate) acid microsphere-encapsulated antigen in vivo. J Immunol 187: 2112–2121. [PubMed: 21795597]
27. Schliehe C, Schliehe C, Thiry M, Tromsdorf UI, Hentschel J, Weller H, and Groettrup M. 2011. Microencapsulation of inorganic nanocrystals into PLGA microsphere vaccines enables their intracellular localization in dendritic cells by electron and fluorescence microscopy. J Control Release 151: 278–285. [PubMed: 21223984]
28. Dou Y, Van Montfoort N, Van Den Bosch A, De Man RA, Zom GG, Krebber W-J, Melief CJM, Buschow SI, and Woltman AM. 2018. HBV-Derived Synthetic Long Peptide Can Boost CD4+ and CD8+ T-Cell Responses in Chronic HBV Patients Ex Vivo. The Journal of Infectious Diseases 217: 827–839. [PubMed: 29220492]
29. Dou Y, Jansen DTSL, Van Den Bosch A, De Man RA, Van Montfoort N, Araman C, Van Kasteren SI, Zom GG, Krebber W-J, Melief CJM, Woltman AM, and Buschow SI. 2020. Design of TLR2-ligand-synthetic long peptide conjugates for therapeutic vaccination of chronic HBV patients. Antiviral Research 178: 104746. [PubMed: 32081741]

30. Shen L, Sigal LJ, Boes M, and Rock KL. 2004. Important Role of Cathepsin S in Generating Peptides for TAP-Independent MHC Class I Crosspresentation In Vivo. Immunity 21: 155–165. [PubMed: 15308097]

31. Shen H, Ackerman AL, Cody V, Giodini A, Hinson ER, Cresswell P, Edelson RL, Saltzman WM, and Hanlon DJ. 2006. Enhanced and prolonged cross-presentation following endosomal escape of exogenous antigens encapsulated in biodegradable nanoparticles. Immunology 117: 78–88. [PubMed: 16423043]

32. Kovacsovics-Bankowski M, and Rock KL. 1994. Presentation of exogenous antigens by macrophages: analysis of major histocompatibility complex class I and II presentation and regulation by cytokines. Eur J Immunol 24: 2421–2428. [PubMed: 7925570]

33. Karttunen J, Sanderson S, and Shastri N. 1992. Detection of rare antigen-presenting cells by the lacZ T-cell activation assay suggests an expression cloning strategy for T-cell antigens. Proc Natl Acad Sci U S A 89: 6020–6024. [PubMed: 1378619]

34. Fuertes Marraco SA, Grosjean F, Duval A, Rosa M, Lavanchy C, Ashok D, Haller S, Otten LA, Steiner QG, Descombes P, Luber CA, Meissner F, Mann M, Szeles L, Reith W, and Acha-Orbea H. 2012. Novel murine dendritic cell lines: a powerful auxiliary tool for dendritic cell research. Front Immunol 3: 331. [PubMed: 23162549]

35. Sanjana NE, Shalem O, and Zhang F. 2014. Improved vectors and genome-wide libraries for CRISPR screening. Nat Methods 11: 783–784. [PubMed: 25075903]

36. Basta S, Stoessel R, Basler M, van den Broek M, and Groettrup M. 2005. Cross-presentation of the long-lived lymphocytic choriomeningitis virus nucleoprotein does not require neosynthesis and is enhanced via heat shock proteins. J Immunol 175: 796–805. [PubMed: 16002676]

37. Houde M, Bertholet S, Gagnon E, Brunet S, Goyette G, Laplante A, Princiotta MF, Thibault P, Sacks D, and Desjardins M. 2003. Phagosomes are competent organelles for antigen cross-presentation. Nature 425: 402–406. [PubMed: 14508490]

38. Grotzke JE, Kozik P, Morel JD, Impens F, Pietrosemoli N, Cresswell P, Amigorena S, and Demangel C. 2017. Sec61 blockade by mycolactone inhibits antigen cross-presentation independently of endosome-to-cytosol export. Proc Natl Acad Sci U S A 114: E5910–E5919. [PubMed: 28679634]

39. Wu T, Guan J, Handel A, Tscharke DC, Sidney J, Sette A, Wakim LM, Sng XYX, Thomas PG, Croft NP, Purcell AW, and La Gruta NL. 2019. Quantification of epitope abundance reveals the effect of direct and cross-presentation on influenza CTL responses. Nature Communications 10.

40. Rock KL, Gramm C, Rothstein L, Clark K, Stein R, Dick L, Hwang D, and Goldberg AL. 1994. Inhibitors of the proteasome block the degradation of most cell proteins and the generation of peptides presented on MHC class I molecules. Cell 78: 761–771. [PubMed: 8087844]

41. Rock KL, and Goldberg AL. 1999. Degradation of cell proteins and the generation of MHC class I-presented peptides. Annu Rev Immunol 17: 739–779. [PubMed: 10358773]

42. Helms JB, and Rothman JE. 1992. Inhibition by brefeldin A of a Golgi membrane enzyme that catalyses exchange of guanine nucleotide bound to ARF. Nature 360: 352–354. [PubMed: 1448152]

43. Norbury CC, Hewlett LJ, Prescott AR, Shastri N, and Watts C. 1995. Class I MHC presentation of exogenous soluble antigen via macropinocytosis in bone marrow macrophages. Immunity 3: 783–791. [PubMed: 8777723]

44. Cruz FM, Colbert JD, and Rock KL. 2020. The GTPase Rab39a promotes phagosome maturation into MHC-I antigen-presenting compartments. EMBO J 39: e102020. [PubMed: 31821587]

45. Cruz-Leal Y, Grubaugh D, Nogueira CV, Lopetegui-González I, del Valle A, Escalona F, Laborde RJ, Alvarez C, Fernández LE, Starnbach MN, Higgins DE, and Lanio ME. 2018. The Vacuolar Pathway in Macrophages Plays a Major Role in Antigen Cross-Presentation Induced by the Pore-Forming Protein Sticholysin II Encapsulated Into Liposomes. Front Immunol 9.

46. Arasaki K, and Roy CR. 2010. Legionella pneumophila promotes functional interactions between plasma membrane syntaxins and Sec22b. Traffic 11: 587–600. [PubMed: 20163564]

47. Montealegre S, and van Endert P. 2017. MHC Class I Cross-Presentation: Stage Lights on Sec22b. Trends Immunol 38: 618–621. [PubMed: 28743621]

48. Muntjewerff EM, Meesters LD, and van den Bogaart G. 2020. Antigen Cross-Presentation by Macrophages. Front Immunol 11.

49. Van Dinther D, Veninga H, Iborra S, Borg EGF, Hoogterp L, Olesek K, Beijer MR, Schetters STT, Kalay H, Garcia-Vallejo JJ, Franken KL, Cham LB, Lang KS, Van Kooyk Y, Sancho D, Crocker PR, and Den Haan JMM. 2018. Functional CD169 on Macrophages Mediates Interaction with Dendritic Cells for CD8+ T Cell Cross-Priming. Cell Reports 22: 1484–1495. [PubMed: 29425504]

50. Panyam J, Zhou WZ, Prabha S, Sahoo SK, and Labhasetwar V. 2002. Rapid endo-lysosomal escape of poly(DL-lactide-coglycolide) nanoparticles: implications for drug and gene delivery. The FASEB Journal 16: 1217–1226. [PubMed: 12153989]

51. Hatsuzawa K, Hashimoto H, Hashimoto H, Arai S, Tamura T, Higa-Nishiyama A, and Wada I. 2009. Sec22b is a negative regulator of phagocytosis in macrophages. Mol Biol Cell 20: 4435–4443. [PubMed: 19710423]

52. Becker T, Volchuk A, and Rothman JE. 2005. Differential use of endoplasmic reticulum membrane for phagocytosis in J774 macrophages. PNAS 102: 4022–4026. [PubMed: 15753287]

53. Zhang T, Wong SH, Tang BL, Xu Y, and Hong W. 1999. Morphological and functional association of Sec22b/ERS-24 with the pre-Golgi intermediate compartment. Mol Biol Cell 10: 435–453. [PubMed: 9950687]

54. Ohya T, Miaczynska M, Coskun U, Lommer B, Runge A, Drechsel D, Kalaidzidis Y, and Zerial M. 2009. Reconstitution of Rab- and SNARE-dependent membrane fusion by synthetic endosomes. Nature 459: 1091–1097. [PubMed: 19458617]

55. Weber T, Zemelman BV, Mcnew JA, Westermann B, Gmachl M, Parlati F, Söllner TH, and Rothman JE. 1998. SNAREpins: Minimal Machinery for Membrane Fusion. Cell 92: 759–772. [PubMed: 9529252]

56. McNew JA, Parlati F, Fukuda R, Johnston RJ, Paz K, Paumet F, Sollner TH, and Rothman JE. 2000. Compartmental specificity of cellular membrane fusion encoded in SNARE proteins. Nature 407: 153–159. [PubMed: 11001046]

57. Liu Y, and Barlowe C. 2002. Analysis of Sec22p in endoplasmic reticulum/Golgi transport reveals cellular redundancy in SNARE protein function. Mol Biol Cell 13: 3314–3324. [PubMed: 12221135]

58. Yang B, Gonzalez L Jr., Prekeris R, Steegmaier M, Advani RJ, and Scheller RH. 1999. SNARE interactions are not selective. Implications for membrane fusion specificity. J Biol Chem 274: 5649–5653. [PubMed: 10026182]

59. Low SH, Vasanji A, Nanduri J, He M, Sharma N, Koo M, Drazba J, and Weimbs T. 2006. Syntaxins 3 and 4 are concentrated in separate clusters on the plasma membrane before the establishment of cell polarity. Mol Biol Cell 17: 977–989. [PubMed: 16339081]

60. Bennett MK, Garcia-Arrarás JE, Elferink LA, Peterson K, Fleming AM, Hazuka CD, and Scheller RH. 1993. The syntaxin family of vesicular transport receptors. Cell 74: 863–873. [PubMed: 7690687]

61. Ravichandran V, Chawla A, and Roche PA. 1996. Identification of a Novel Syntaxin- and Synaptobrevin/VAMP-binding Protein, SNAP-23, Expressed in Non-neuronal Tissues. Journal of Biological Chemistry 271: 13300–13303. [PubMed: 8663154]

Key points:

1. We investigated cross-presentation by APCs with homozygous KO for Sec22b and Stx4.
2. To our knowledge, this is the first study directly examining the role of Stx4 in cross-presentation.
3. KO of both Sec22b and Stx4 did not have major impact on the cross-presentation of tested antigens.

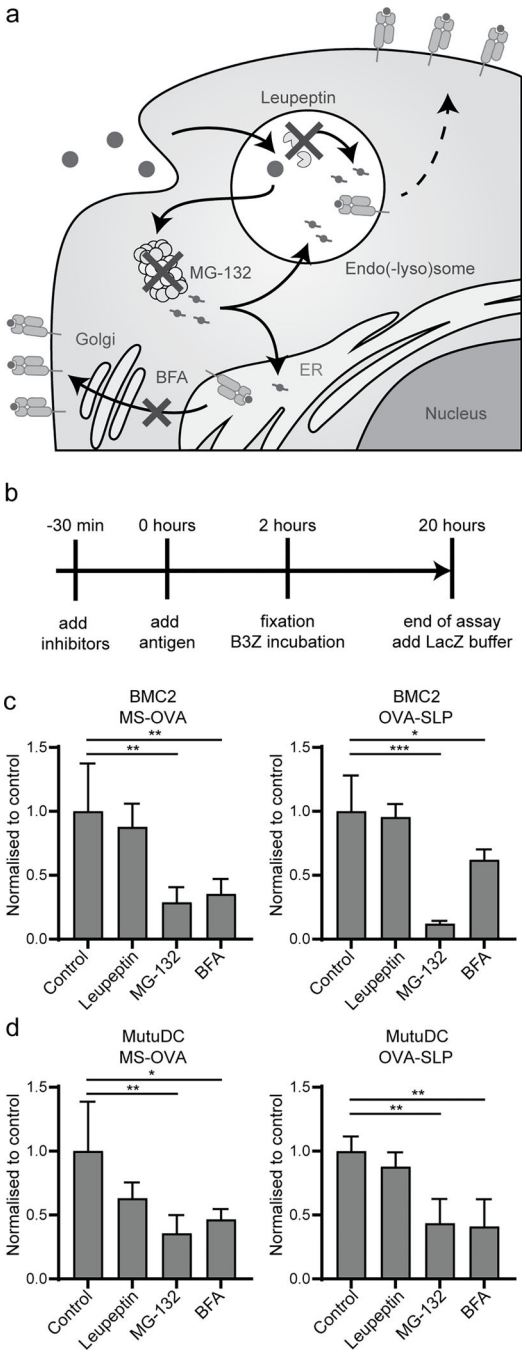

Figure 1. Cross-presentation of OVA-SLP and MS-OVA mainly follows a cytosolic pathway.

a) Graphical illustration of cellular targets of the inhibitors used to interfere with cross-presentation pathways. **b)** Schematic representation of the inhibitor experiment. Antigen presenting cells (APCs) were pre-treated for 30 min with the following inhibitors: 100 μM leupeptin (cathepsin inhibitor), 10 μM MG-132 (proteasome inhibitor), 10 μg/ml Brefeldin A (BFA, inhibits ER to Golgi transport), before incubation with either 25 μg/96-well of PLGA microsphere-encapsulated ovalbumin (OVA) (MS-OVA) or 10 μg/ml of an OVA-derived synthetic long peptide (OVA-SLP). After 2 hours, APCs were fixed with PFA

and cross-presentation was quantified using a B3Z T-cell hybridoma assay. **c+d)** Antigen cross-presentation of MS-OVA (**left panels**) and OVA-SLP (**right panels**) by BMC2 (**c**) and MutuDC cells (**d**). B3Z T-cell activation was evaluated in a colorimetric LacZ assay by measuring the optical density (OD) on an ELISA plate reader (OD_{570nm}-OD_{620nm}). Data was normalized to the respective control condition in the presence of antigen without inhibitor treatment. Pooled results from four independent experiments are shown as mean with standard deviation and each independent experiment was performed with three technical replicates. Statistical evaluation of mean differences was performed using an one-way ANOVA with post-hoc Dunnet's test to compare inhibitor treated samples to the respective control condition, with * = $p < 0.05$; ** = $p < 0.01$; *** = $p < 0.001$.

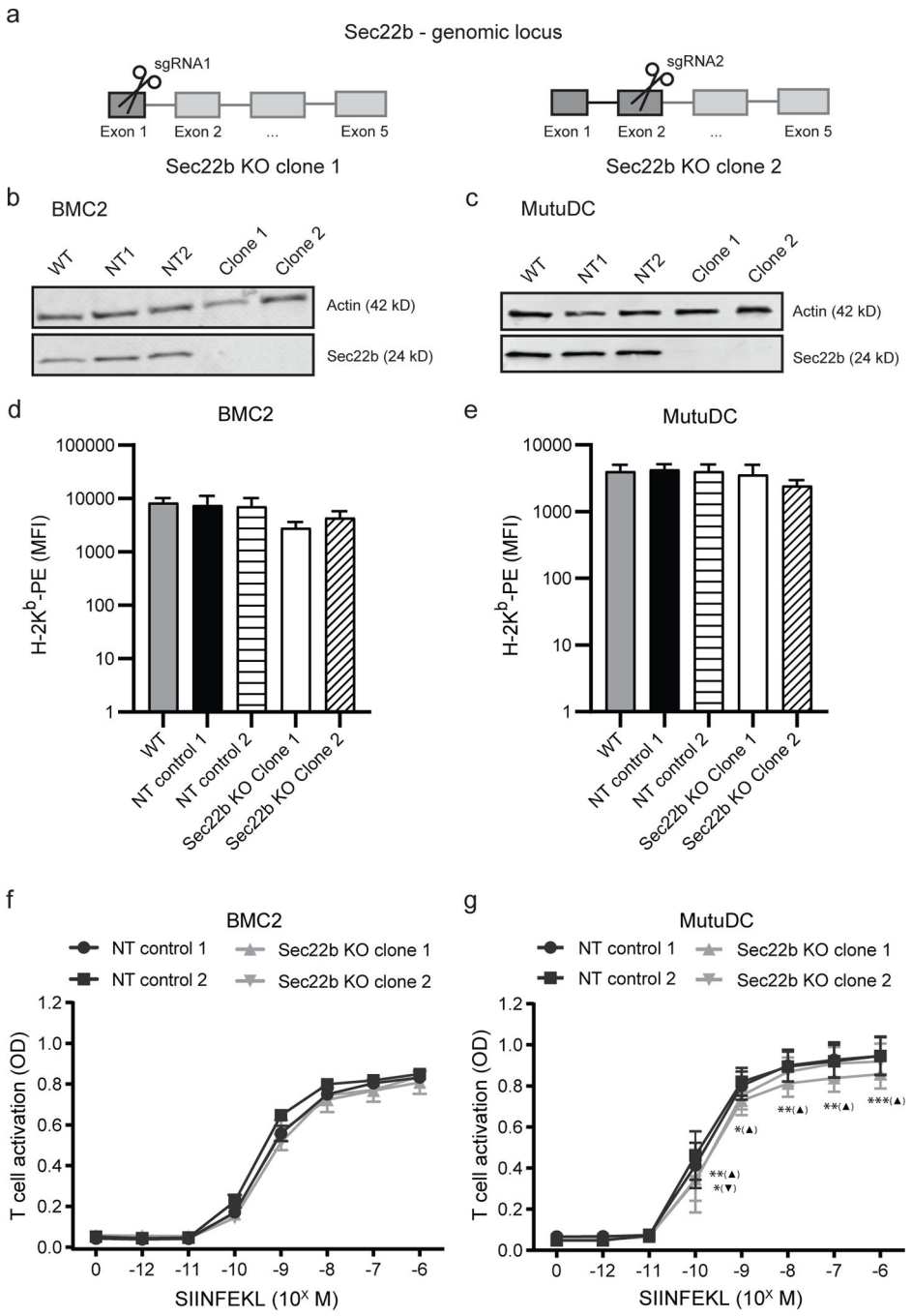

Figure 2. Sec22b knockout does not alter normal surface expression of MHC class I.

a) Graphical illustration of CRISPR/Cas9 gene editing strategy used to generate Sec22b knockout (KO) cells. Antigen presenting cells (APCs) were transduced with lentiviral vectors containing Sec22b-specific single guide RNAs (sgRNA1 and 2) targeting exon 1 and exon 2 of *Sec22b*, respectively, selected for successful viral integration, and further subcloned to obtained single cell-derived KO clones. **b+c)** KO of Sec22b was confirmed on the protein level after cell lysis by western blot analysis using an anti-Sec22b antibody (expected molecular weight ~24kDa) for wildtype (WT), non-targeting sgRNA control 1

(NT1) and 2 (NT2) and Sec22b-targeted cells (sgRNA1 and sgRNA2; Sec22b KO clone 1 and 2, respectively) with BMC2 (**b**) and MutuDC cells (**c**). An anti-actin antibody was used as control for equal protein loading. Western blot shown is representative of three independent experiments. **d+e)** APCs were harvested and stained for H-2K^b to analyse MHC class I surface expression by flow cytometry on BMC2 (**c**) and MutuDC cells (**d**) (gating strategy Supp. Fig 2a). Graphs show median fluorescence intensity (MFI) of the pooled data from three (**c**) or four (**d**) independent experiments, illustrated as mean with standard deviation. Each independent experiment was performed with one technical replicate. **f+g)** BMC2 (**f**) and MutuDC cells (**g**) were externally pulsed with indicated concentrations of the ovalbumin-derived, H-2K^b-restricted T-cell epitope SIINFEKL for 1 hour, washed 3 times, and then co-cultured with B3Z T-cell hybridomas for 18 hours. B3Z T-cell activation was evaluated in a colorimetric LacZ assay by measuring the optical density (OD) on an ELISA plate reader (OD_{570nm}-OD_{620nm}). Graphs show pooled data with mean with standard deviation from six independent experiments with three technical replicates. Statistical evaluation of mean differences was performed using a one-way ANOVA followed by Tukey test (**c-d**) or a two-way ANOVA followed by Tukey test (**e-f**). Results were only indicated as significant if Sec22b KO APCs targeted with either sgRNA1 or sgRNA2 were significantly different from both NT controls, with * = $p < 0.05$; ** = $p < 0.01$; *** = $p < 0.001$.

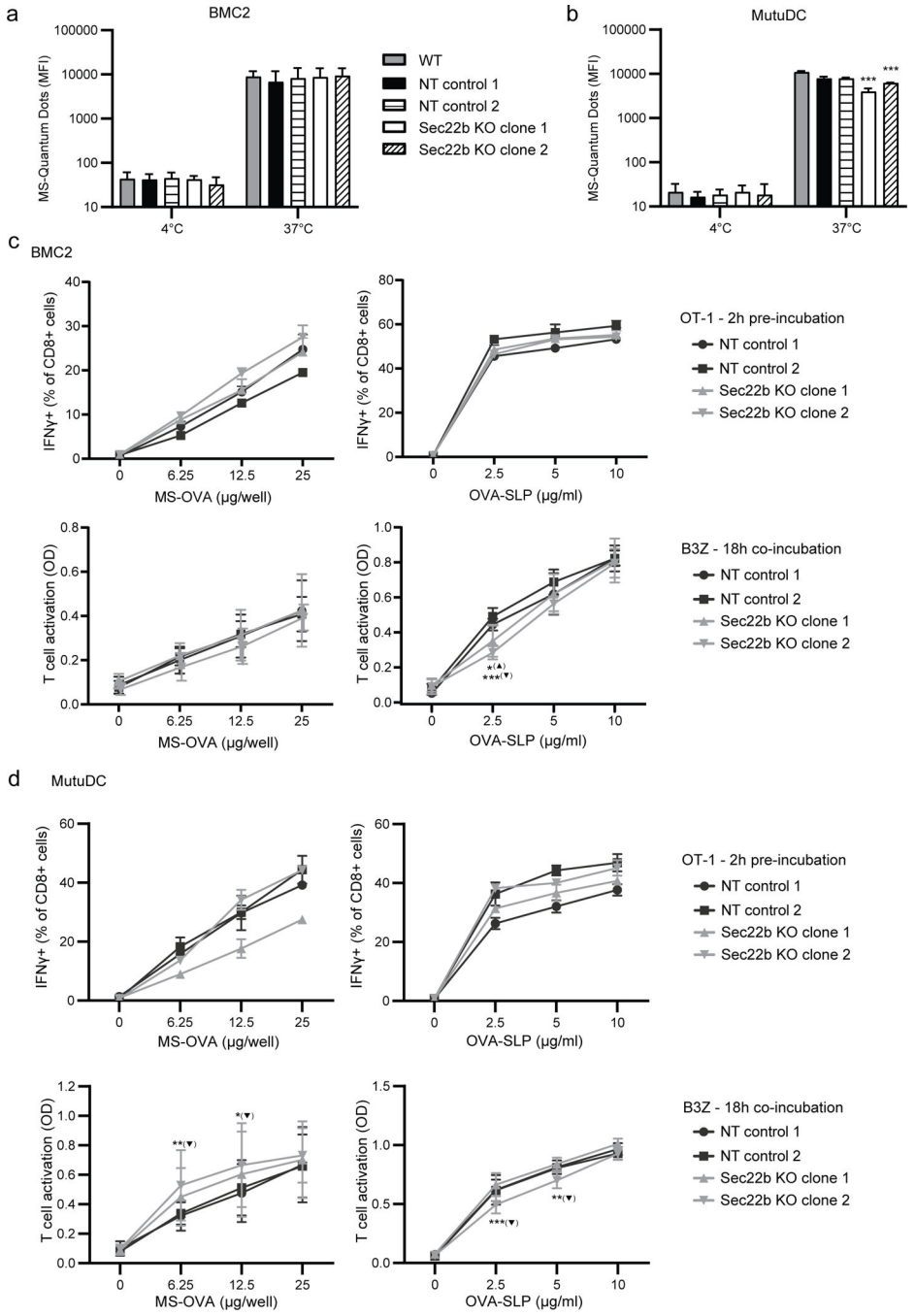

Figure 3. APCs lacking Sec22b efficiently cross-present MS-OVA and OVA-SLP.

a+b) Antigen uptake by BMC2 (**a**) and MutuDC cells (**b**) was evaluated using PLGA microspheres containing fluorescent quantum dots (MS-QD; 583nm; **right panel**). Antigen presenting cells (APCs) were incubated with MS-QD at indicated temperatures for 2 hours before antigen uptake was analyzed by flow cytometry (gating strategy Supp. Fig. 2d). Graphs show median fluorescence intensity (MFI) and display the pooled results of three independent experiments as mean with standard deviation, performed with one technical replicate. **c+d)** Cross-presentation efficiency in Sec22b knockout (KO) BMC2 cells (**c**) and

MutuDC cells (**d**) with indicated concentrations of PLGA microsphere-encapsulated OVA (MS-OVA; **left panels**) or an ovalbumin (OVA)-derived synthetic long peptide (OVA-SLP; **right panels**) for either pre-incubation of 2 hours with the antigen followed by addition of primary OT-1 T-cells for 4 hours in presence of brefeldin A (**top panels**) or co-incubation of 18 hours in the presence of B3Z hybridoma cells (**bottom panels**). APCs transduced with non-targeting sgRNAs (NT control 1 and 2) were used as control. Primary OT-1 T-cell activation was evaluated by intracellular cytokine staining for IFN-γ followed by flow cytometry. Graphs show the mean percentage of IFN-γ positive events from the total population of $CD8^+$ T-cells. One representative of three independent experiments with standard deviation is shown (gating strategy Suppl. Fig. 2c). Each independent experiment was performed with two technical replicates. B3Z T-cell activation was evaluated in a colorimetric LacZ assay by measuring the optical density (OD) on an ELISA plate reader (OD_{570nm}-OD_{620nm}). Graphs show the pooled data as mean with standard deviation from five (**c**, **bottom left**) or three (**c**, **bottom right + d**, **bottom right**) or seven (**d**, **bottom left**) independent experiments. All independent experiments were performed with three technical replicates. Statistical evaluation of mean differences was performed on pooled data from all replicates using a one-way ANOVA followed by Tukey test on the 37°C phagocytosis condition (**a+b**) or by a two-way ANOVA followed by Tukey test (**c+d**). Results were indicated as significant if KO APCs targeted with either sgRNA1 or sgRNA2 were significantly different from both NT controls, with * = $p < 0.05$; ** = $p < 0.01$; *** = $p < 0.001$.

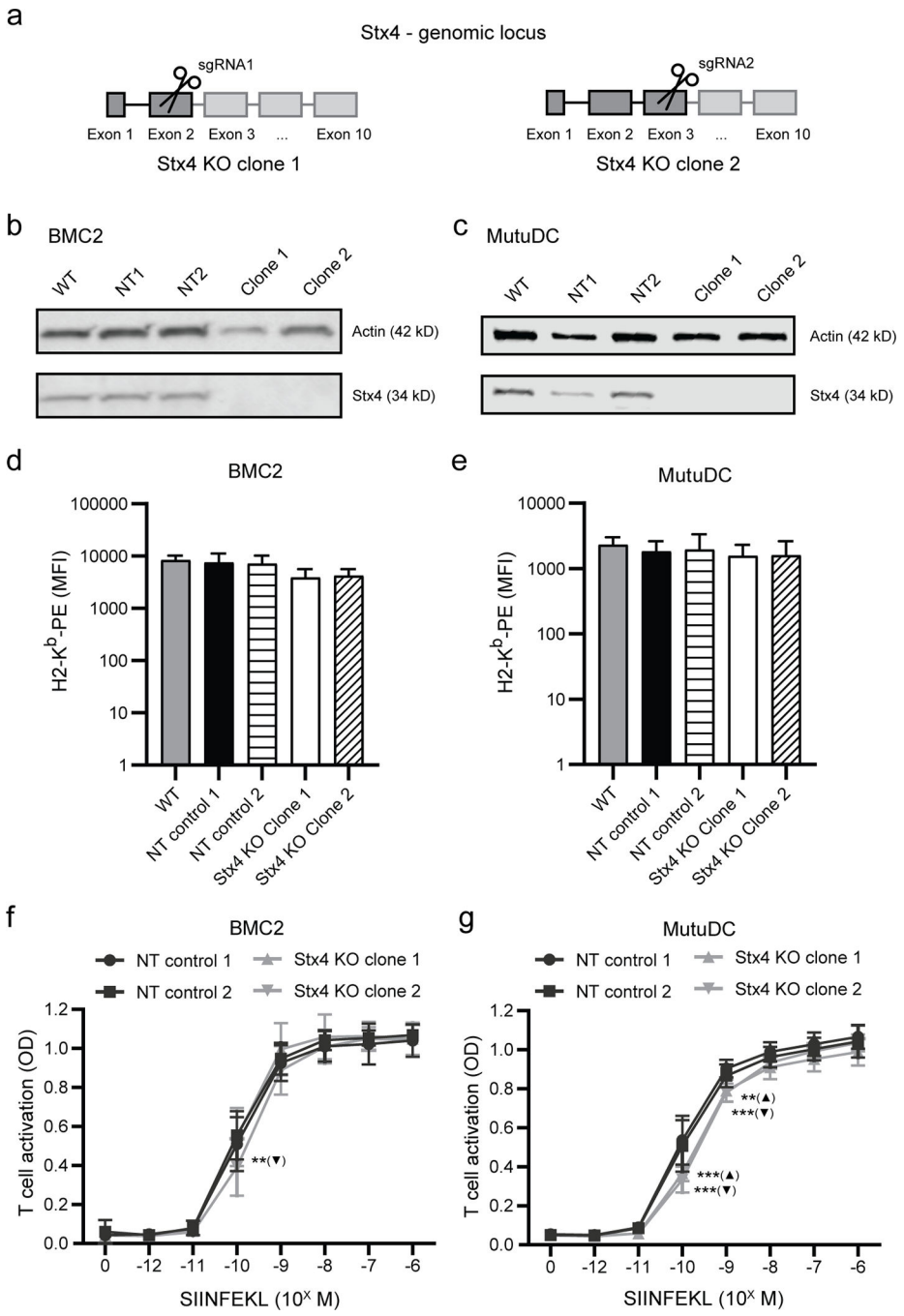

Figure 4. Stx4 knockout does not affect MHC class I surface expression on both BMC2 and MutuDC cells.

a) Graphical illustration of CRISPR/Cas9 gene editing strategy used to generate Stx4 knockout (KO) cells. Antigen presenting cells (APCs) were transduced with lentiviral vectors containing Stx4-specific single guide RNAs (sgRNA1 and 2) targeting exon 2 and exon 3 of *Stx4*, respectively, selected for successful viral integration, and further subcloned to obtained single cell-derived KO clones. **b-c)** KO of Stx4 was confirmed on the protein level after cell lysis by western blot analysis using an anti-Stx4 antibody

(expected molecular weight ~34kDa) for wildtype (WT), non-targeting sgRNA control 1 (NT1) and 2 (NT2) and Stx4-targeted cells (sgRNA1 and sgRNA2; Stx4 KO clone 1 and 2, respectively) with BMC2 (**b**) and MutuDC cells (**c**). An anti-actin antibody was used as control for equal protein loading. Western blot shown is representative of two independent experiments. **d+e)** APCs were harvested and stained for H-2K^{b} to analyze MHC class I surface expression by flow cytometry on BMC2 (**d**) and MutuDC cells (**e**). Graphs show median fluorescence intensity (MFI) of the pooled data from four (**d**) or three (**e**) independent experiments, illustrated as mean with standard deviation (gating strategy Suppl. Fig. 2a). Each independent experiment was performed with one technical replicate. **f+g)** BMC2 (**f**) and MutuDC cells (**g**) were externally pulsed with indicated concentrations of the ovalbumin-derived, H-2K^{b}-restricted T-cell epitope SIINFEKL for 1 hour, washed 3 times, and then co-cultured with B3Z T-cell hybridomas for 18 hours. B3Z T-cell activation was evaluated in a colorimetric LacZ assay by measuring the optical density (OD) on an ELISA plate reader (OD_{570nm}-OD_{620nm}). Graphs show the pooled data as mean with standard deviation from four (**f+g**) independent experiments. Each independent experiment was performed with three technical replicates. Statistical evaluation of mean differences was performed using a one-way ANOVA followed by Tukey multiple comparisons test (**c-d**) or a two-way ANOVA followed by Tukey test (**e-f**). Results were indicated as significant if Stx4 KO APCs targeted with either sgRNA1 or sgRNA2 were significantly different from both NT controls, with * = $p < 0.05$; *** = $p < 0.001$.

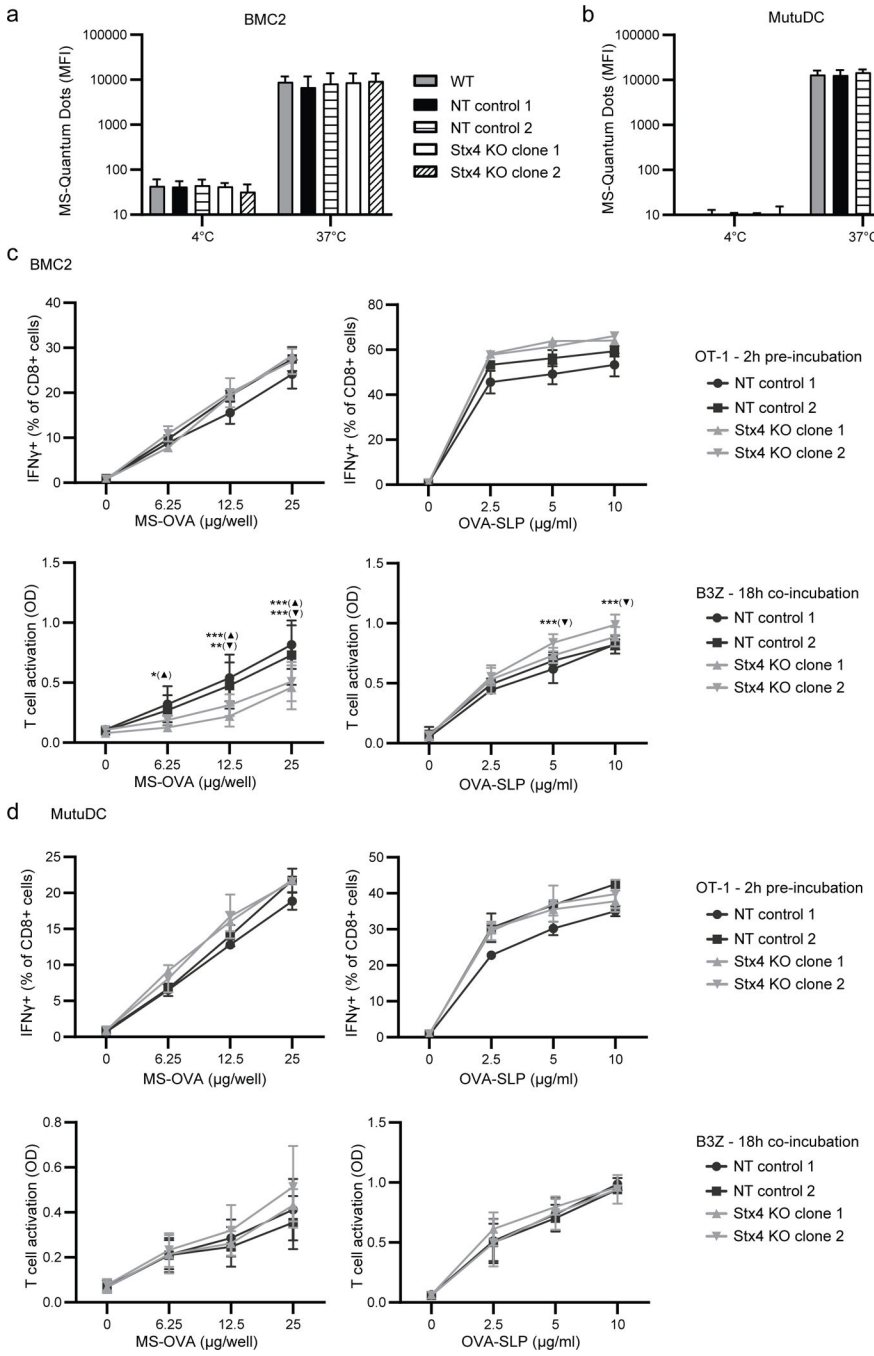

Figure 5. Stx4 KO has no major effect on cross-presentation of OVA-SLP and MS-OVA.

a+b) Antigen uptake by BMC2 (**a**) and MutuDC cells (**b**) was evaluated using PLGA microspheres containing fluorescent quantum dots (MS-QD; 583nm). Antigen presenting cells (APCs) were incubated with MS-QD at indicated temperatures for 2 hours before antigen uptake was analyzed by flow cytometry (gating strategy Suppl. Fig. 2d). Graphs show median fluorescence intensity (MFI) and summarize the results of three independent experiments as mean with standard deviation. Each independent experiment was performed with one technical replicate. **c+d)** Cross-presentation efficiency in Stx4 knockout (KO)

BMC2 cells (**c**) and MutuDC cells (**d**) with indicated concentrations of PLGA microsphere-encapsulated OVA (MS-OVA; **left panels**) or an ovalbumin (OVA)-derived synthetic long peptide (OVA-SLP; **right panels**) for either 2 hours of pre-incubation with the antigen followed by addition of primary OT-1 T-cells for 4 hours in presence of brefeldin A (**top panels**) or co-incubation of 18 hours in the presence of B3Z hybridoma cells (**bottom panels**). APCs transduced with non-targeting sgRNAs (NT control 1 and 2) were used as control. Primary OT-1 T-cell activation was evaluated by intracellular cytokine staining for IFN-γ followed by flow cytometry. Graphs show the mean percentage of IFN-γ positive events from the total population of $CD8^+$ T-cells from one representative of three independent experiments with standard deviation (gating strategy Suppl. Fig. 2c). Each independent experiment was performed with two technical replicates. B3Z T-cell activation was evaluated in a colorimetric LacZ assay by measuring the optical density (OD) on an ELISA plate reader (OD_{570nm}-OD_{620nm}). Graphs show the pooled data as mean with standard deviation from three (**c, bottom right**; **d, bottom panels**) or five (**c, bottom left**) independent experiments. Each independent experiment was performed with three technical replicates. Statistical evaluation of mean differences was performed on pooled data using a one-way ANOVA followed by Tukey test on the 37°C condition (**a+b**) or by a two-way ANOVA followed by Tukey post-hoc test (**c+d**). Results were indicated as significant if KO APCs targeted with either sgRNA1 or sgRNA2 were significantly different from both NT controls, with * = $p < 0.05$; ** = $p < 0.01$; *** = $p < 0.001$.